




Robust Archaeal and Bacterial Communities Inhabit Shallow Subsurface Sediments of the Bonneville Salt Flats

Julia M. McGonigle,^a Jeremiah A. Bernau,^b Brenda B. Bowen,^b  William J. Brazelton^a

^aSchool of Biological Sciences, University of Utah, Salt Lake City, Utah, USA

^bDepartment of Geology and Geophysics, University of Utah, Salt Lake City, Utah, USA

ABSTRACT We report the first census of natural microbial communities of the Bonneville Salt Flats (BSF), a perennial salt pan at the Utah-Nevada border. Environmental DNA sequencing of archaeal and bacterial 16S rRNA genes was conducted on samples from multiple evaporite sediment layers collected from the upper 30 cm of the surface salt crust. Our results show that at the time of sampling (September 2016), BSF hosted a robust microbial community dominated by diverse halobacteria and *Salinibacter* species. Sequences identical to *Geitlerinema* sp. strain PCC 9228, an anoxygenic cyanobacterium that uses sulfide as the electron donor for photosynthesis, are also abundant in many samples. We identified taxonomic groups enriched in each layer of the salt crust sediment and revealed that the upper gypsum sediment layer found immediately under the uppermost surface halite contains a robust microbial community. In these sediments, we found an increased presence of *Thermoplasmatales*, *Hadesarchaeota*, *Nanoarchaeaeota*, *Acetothermia*, *Desulfovermiculus*, *Halanaerobiales*, *Bacteroidetes*, and *Rhodovibrio*. This study provides insight into the diversity, spatial heterogeneity, and geologic context of a surprisingly complex microbial ecosystem within this macroscopically sterile landscape.

IMPORTANCE Pleistocene Lake Bonneville, which covered a third of Utah, desiccated approximately 13,000 years ago, leaving behind the Bonneville Salt Flats (BSF) in the Utah West Desert. The potash salts that saturate BSF basin are extracted and sold as an additive for agricultural fertilizers. The salt crust is a well-known recreational and economic commodity, but the biological interactions with the salt crust have not been studied. This study is the first geospatial analysis of microbially diverse populations at this site using cultivation-independent environmental DNA sequencing methods. Identification of the microbes present within this unique, dynamic, and valued sedimentary evaporite environment is an important step toward understanding the potential consequences of perturbations to the microbial ecology on the surrounding landscape and ecosystem.

KEYWORDS astrobiology, extremophiles, halophiles, hypersaline environments

The Great Salt Lake and Bonneville Salt Flats (BSF) are both remnants of Pleistocene Lake Bonneville which partially drained at the end of the last glacial maximum and desiccated ~13,000 years ago (1). BSF is famous for its use as a speedway through the last century, which has hosted many land-speed records and a community that greatly values this saline landscape (2). Over this same time period, the salts that saturate BSF basin have been extracted as an economic commodity, particularly as potash (e.g., KCl) that is sold as an additive for agricultural fertilizers. The hydrology and sedimentology of BSF have been studied periodically throughout the 20th century in relation to potash mining and concerns about the impacts of land use on the environment (3–9). Human land use has altered many aspects of the hydrology and morphology of the environment that facilitated deposition of the ~2-m-thick evaporite lens-shaped crust that

Citation McGonigle JM, Bernau JA, Bowen BB, Brazelton WJ. 2019. Robust archaeal and bacterial communities inhabit shallow subsurface sediments of the Bonneville Salt Flats. *mSphere* 4:e00378-19. <https://doi.org/10.1128/mSphere.00378-19>.

Editor Hideyuki Tamaki, National Institute of Advanced Industrial Science and Technology, Japan

Copyright © 2019 McGonigle et al. This is an open-access article distributed under the terms of the [Creative Commons Attribution 4.0 International license](https://creativecommons.org/licenses/by/4.0/).

Address correspondence to Julia M. McGonigle, j.mcgonigle@utah.edu.

Received 28 May 2019

Accepted 12 August 2019

Published 28 August 2019

caps BSF. The amount and extent of salt present at the site have been observed to fluctuate and decrease through the past century (10, 11).

Examination of modern and ancient salt pan deposits demonstrates that these environments undergo repeated cycles of desiccation (dry saline pan), flooding (brackish lake), and evaporative concentration (drying to dry saline pan) (12, 13). The desiccation stage is repeatedly interrupted by flooding events related to individual storms, wet seasons, and spring thaws driving runoff from surrounding mountains. The environmental parameters that influence the hydrology and timing of flooding, evaporation, and desiccation cycles are dynamic (14). For this study, multiple individual strata from several sites spanning the salt crust were sampled at BSF during an extensive sampling campaign to measure the overall stratigraphy and volume of the salt crust (11). The samples were collected in early September 2016 near the end of a 3-month desiccation period.

Microbial communities provide critical ecosystem services by cycling nutrients and providing a biological foundation upon which other organisms can establish themselves. In environments considered “extreme” by human standards such as BSF, microbes are often the only life forms that can survive. The study of microbial life in these ecosystems can elucidate how extremophilic organisms have evolved unique attributes, strategies, and metabolic capabilities that enable them to thrive where most other organisms cannot (15, 16). Extreme hypersaline ecosystems select for organisms capable of not only tolerating, but actually requiring high levels of salt for growth (17). Microbes in these ecosystems employ either a “salt-in” or “organic-solutes-in” strategy to overcome the problems associated with osmoregulation in a high-salt environment (18). In addition, halophiles found in these environments produce enzymes with potential biotechnological, bioremediation, and medical applications (19).

The role of microbes in BSF salt crust processes are generally unknown. Identification of the microbes present within this unique, dynamic, and valued evaporite environment is an important step toward understanding the potential consequences of perturbations to the microbial ecology on the surrounding landscape and ecosystem. This study is the first geospatial analysis of microbially diverse populations at BSF using cultivation-independent environmental DNA sequencing methods. This study provides insight into the diversity, spatial heterogeneity, and geologic context of a surprisingly complex microbial ecosystem within this macroscopically sterile landscape.

RESULTS

Elemental and sedimentological analysis. Thin sections and reconstructed mineralogy from elemental data were used to group each sample into one of four classifications: group 1 (surface halite), group 2 (upper gypsum), group 3 (lower halite), and group 4 (halite mixed with gypsum).

Elemental analysis and thin section microscopy reveal layers of distinct sedimentological morphology (Fig. 1; see also Fig. S2 in the supplemental material). Primary minerals were identified as halite (NaCl), gypsum ($\text{CaSO}_4 \cdot 2\text{H}_2\text{O}$), and clay and detrital minerals (Fe, Mg, and Al). The majority of samples were above reporting limits for sodium. All minerals are reported as weight % of composition (see Data Set S1 in the supplemental material). The relative enrichment of select major and trace elements was determined for each sediment classification (Table 1). Groups with mean values above the cutoff limit were reported as enriched with an element.

Thin sections revealed group 1 (surface halite) consists of puffy fine efflorescent halite crystals, followed by larger halite crystals (up to 0.5 cm wide) with fluid inclusions. Group 1 samples are composed of predominantly halite with gypsum (2.5 to 27%) and trace amounts (<0.5%) of clay. Group 1 is relatively enriched in chloride, potassium, and zinc (from most to least abundant).

Group 2 (upper gypsum) consists of layered fine to medium sized gypsum grains. Group 2 samples contain gypsum (29 to 39%) and halite (6 to 22%). Group 2 samples contain the largest amount of clay and detrital minerals of any strata (0.3 to 1.7%). Reconstructed mineralogy only accounted for 41 to 61% of group 2's mass. Group 2 is

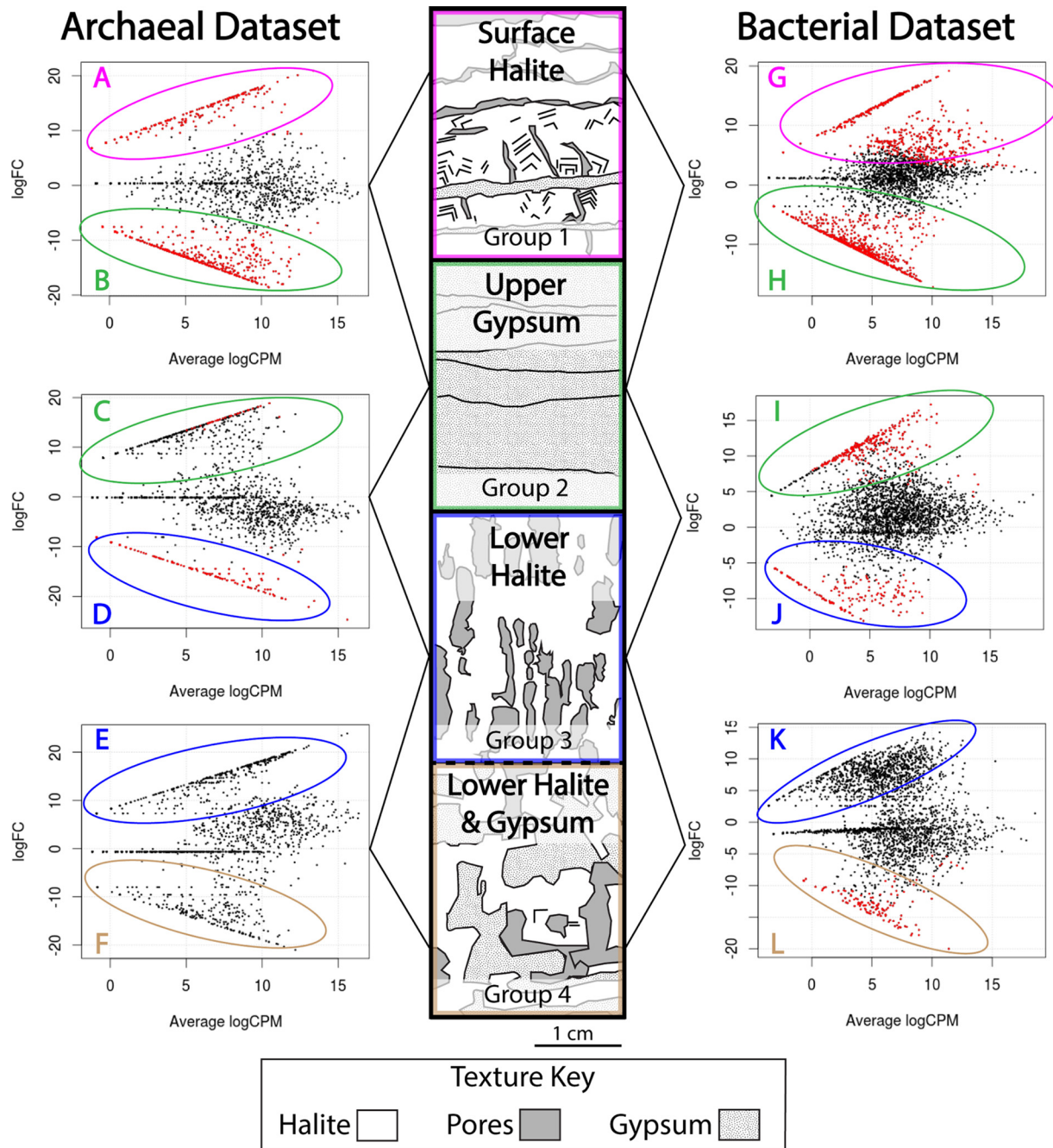


FIG 1 Sedimentology and differential abundance results (edgeR) for archaeal and bacterial data sets. Red dots indicate an ASV with a significantly higher abundance ($FDR < 0.05$) in the indicated category. Representative stratigraphic columns are presented here. Dashed lines represent stratigraphic shifts that only occurred at some sites. General stratigraphy consists of groups 1 to 5. Group 1, surface halite, contains efflorescent halite and halite crystals with abundant fluid inclusions. Group 2, upper gypsum, consists of gypsum grains with various proportions of halite; this group has the highest proportion of clays. Group 3, lower halite, has the highest proportion of pore space and is mineralogically similar to group 1. Group 4, lower halite and gypsum, forms when pores in lower halite fill with gypsum. Axis abbreviations: logFC, \log_2 -fold change (differential abundance); logCPM, \log_2 counts per million across all samples in comparison.

enriched in sulfur, calcium, magnesium, aluminum, potassium, iron, strontium, zinc, barium, and manganese.

Group 3 (lower halite) samples are cemented halite with porous vertical dissolution pipes. These pipes are typically 10 to 30 mm wide, but some are >1 cm. Elemental data from group 3 are similar to the data from group 1 (surface halite). Group 3 is enriched in chloride and zinc.

TABLE 1 Sample means for sediment categories^a

Element	Cutoff value	Sample mean for group:			
		1	2	3	4
Cl	450,000 mg/liter	541,125	70,342.86	546,000	383,000
Sr	200 ppm	106.375	533	122.8	449.25
Zn	10 ppm	47.5	81.28571	40.2	11.5
Mn	15 ppm	10.25	37.85714	9.2	10.25
Ba	20 ppm	1.75	31.14286	4.6	19
Ca	5%	1.9925	8.867143	2.376	6.8675
S	2%	1.5375	6.435714	1.824	5.9275
Mg	0.20%	0.12625	0.422857	0.086	0.1425
K	0.15%	0.19625	0.204286	0.112	0.1325
Al	0.10%	0.01375	0.157143	0.022	0.045
Fe	0.05%	0.02	0.138571	0.026	0.0425

^aBoldface values indicate that an element is enriched in samples.

Group 4 (halite mixed with gypsum) consists of a chaotic halite supported framework (53 to 61%) made from vestigial dissolution pipes filled by pore space and gypsum (28 to 33%). Group 4 is enriched in calcium, sulfur, strontium, and zinc.

Bacterial and archaeal community composition. All sediment samples produced 1,845,510 merged paired reads with the bacterial primer set and 552,906 merged paired reads with the archaeal primer set. From these, DADA2 identified 2,740 amplicon sequence variants (ASVs) in the bacterial data set and 1,646 ASVs in the archaeal data set. DNA extraction yields and ASV counts per sample are shown in Table S1 in the supplemental material. These ASV counts were transformed with the DNA extraction yields with the procedure described in the methods to obtain biomass-weighted environmental abundances for downstream analyses. At most sites, the samples in groups 1 and 2 have higher DNA yields and ASV counts than the samples from group 3 or group 4. Samples from groups 1 and 2 were sequenced more successfully than those in other groups, particularly with archaeal primers.

There were 1,552 ASVs (56% of the total ASVs) in the bacterial data set that were assigned archaeal taxonomy. The 515F/806R bacterial primers are known to amplify both bacteria and archaea, so we chose to include the archaeal ASVs in the bacterial data set rather than remove such a large proportion of the total sequence diversity (20–22). Most archaeal ASVs in the bacterial data set overlap classifications found in the archaeal data set, but the archaeal data set generally provided more specific classifications, particularly for the class *Thermoplasmata*.

All samples are dominated by *Halobacteria* from six different families (*Haloadaptaceae*, *Halobacteriaceae*, *Halococcaceae*, *Haloferacaceae*, *Halomicrobiaceae*, and J07HX5) and *Salinibacter* species (Fig. S3). Sequences most closely related to *Geitlerinema* sp. strain PCC 9228 and *Deltaproteobacteria* from the families *Bradymonadaceae* and *Desulfohalobiaceae* were also abundant in many samples. Less-dominant taxa generally increase in abundance with depth at most sites.

All samples in the archaeal data set are dominated by *Halobacteria* from 34 different classified genera (Fig. S4). *Haloferacaceae* and *Halomicrobiaceae* are the most abundant families. *Halapricum* and *Halomicroarcula* (both in *Halomicrobiaceae*) are the most dominant genera among the *Halobacteria*. ASVs classified to *Halobacteriales* from the family J07HX5 appear to be more abundant in the upper sediments. ASVs classified as *Halosulfurarchaeum* appear to be higher in relative abundance in upper gypsum samples. Sequences related to *Hadesarchaeaeota*, *Nanohaloarchaeia* (particularly from *Aenigmarchaeales*), *Bathyarchaeia*, *Thermoplasmata*, and *Methanomicrobia* appear to be more abundant in lower layers.

The ASVs in the bacterial data set were classified as belonging to *Halobacteria* representing 31 genera. As in the archaeal data set, *Haloferacaceae* and *Halomicrobiaceae* are the most abundant families and *Halapricum* and *Halomicroarcula* (both in *Halomicrobiaceae*) were the most dominant genera across all samples. In this data set, however, it appears that *Halomicroarcula* decreases in relative abundance with the

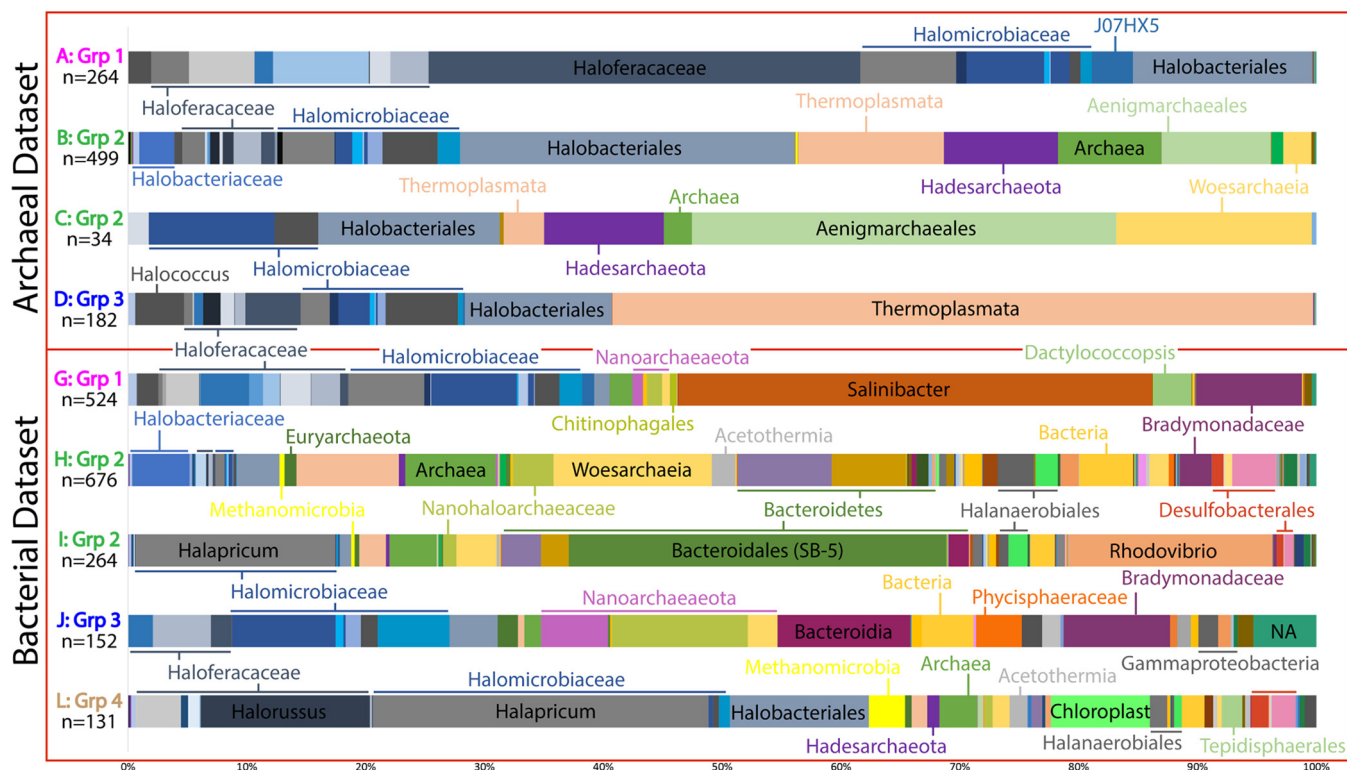


FIG 2 Abundances of ASVs enriched in each group, as determined by the differential abundance (edgeR) comparisons shown in Fig. 1. The numbers of ASVs making up the total plot are indicated below the comparison ID. A full legend can be found in Fig. S6.

depth of the sample. *Halorussus*, *Halorubellus*, and unclassified *Halobacteriales*, on the other hand, increase in relative abundance with the depth of the sample.

The most dominant ASVs related to cyanobacteria are classified as *Geitlerinema* sp. PCC 9228 and are more abundant in upper surface halite and upper gypsum layers. The relative abundances of *Acetothermia*, *Marinilabiaceae* (and other *Bacteroidales*), *Desulfovermiculus*, *Gemmatimonadetes*, *Phycisphaeraceae*, and *Thiohalorhabdus* are greater in lower layers.

Multivariate analysis of the beta diversity for the bacterial and archaeal data sets did not reveal any significant correlations between community compositions and location or sediment depth. (Fig. S5). Similarly, the alpha diversity, as measured by the Simpson index, did not exhibit any consistent patterns with location or sediment depth (Table S2). These results highlight the general lack of significant variation among the whole-community compositions prior to differential abundance analyses.

Differential abundance. Despite the lack of variation at a whole community level, we investigated whether specific ASVs are significantly enriched in one or more sediment classifications. Differential abundances of ASVs were calculated with edgeR (23) by comparing each of the sediment groups to each other (Fig. 1). For both data sets, comparisons were made between groups 1 and 2, between groups 2 and 3, and between groups 3 and 4. All comparisons were made with at least two samples per group.

In the bacterial data set, comparisons between groups 1 and 2 identified 524 ASVs, with significantly greater abundance (determined by a false discovery rate [FDR] of <0.05) in group 1 (surface halite), and 676 ASVs, with significantly greater abundance in group 2 (upper gypsum) (Fig. 2; see also Fig. S6). Diverse *Halobacteria* are the most abundant of the surface halite-enriched ASVs (41%). *Salinibacter* species are also highly abundant among the surface halite-enriched ASVs (40%). The remaining ASVs enriched in group 1 are related to the cyanobacteria *Dactylococcopsis* sp. strain PCC-8305, *Bradymonadaceae*, *Nanohaloarchaeota*, and unclassified members of *Chitinophagales*

and *Archaea*. The enriched taxa become more diverse as the sediment transitions from surface halite to the upper gypsum layer. Taxa with a greater abundance in these group 2 sediments include *Thermoplasmata*, *Nanohaloarchaeaceae*, *Woesearchaeia*, *Acetothermia*, *Halanaerobium*, *Desulfovermiculus*, *Thiohalorhabdus*, *Parcubacteria*, *Planctomycetes*, *Gemmatimonadetes*, *Marinilabiaceae*, and other *Bacteroidetes*. *Methanomicrobia* are also more enriched in upper gypsum sediments, as well as unclassified bacterial and archaeal ASVs.

In the archaeal data set, comparisons between groups 1 and 2 identified 264 ASVs, with significantly higher abundance in group 1 (surface halite), and 499 ASVs, with significantly higher abundance in group 2 (upper gypsum). Diverse *Halobacteria* make up 99% of the abundance of the surface halite-enriched ASVs in samples from this group, with the majority of these related to *Haloferaceae*. The remaining enriched ASVs in group 1 belong to members of deep-sea euryarchaeotal groups (DSEG) and *Thaumarchaeota*. The ASVs enriched in group 2 are dominated by diverse *Halomicrobiaceae* and unclassified *Halobacteriales*. Other highly abundant upper gypsum-enriched ASVs grouped most closely with *Thermoplasmata*, *Hadesarchaeota*, *Aenigmarchaeales*, and unclassified *Archaea*.

The numbers of enriched ASVs identified by differential abundance comparisons between upper gypsum and deeper sediment layers are much lower. In the bacterial data set, comparing group 2 (upper gypsum) and 3 (lower halite) revealed 264 enriched ASVs in group 2, mostly from *Halapricum*, *Bacteroidetes* (specifically from the SB-5 group), and *Rhodovibrio*. Less-abundant upper gypsum-enriched ASVs include *Desulfobacterales*, *Methanomicrobia*, *Nanohaloarchaeaceae*, *Woesearchaeia*, *Halanerobiales*, and unclassified *Bacteria* and *Archaea*. The comparison found 152 group 3-enriched ASVs. The enriched *Halobacteria* in these sediments are heavily represented by *Halomicrobiaceae*. The other abundant lower halite-enriched ASVs are most closely related to *Nanoarchaeaeota*, *Bacteroidia*, *Phycisphaeraceae*, and *Bradymonadaceae*. *Coxiella* and other unclassified *Gammaproteobacteria* are also more enriched in these group 3 sediments.

In the archaeal data set, comparisons between groups 2 (upper gypsum) and 3 (lower halite) found only 34 ASVs that were more abundant in group 2 samples. The most abundant enriched ASVs were classified as *Aenigmarchaeales* and *Woesearchaeia*. Other upper gypsum-enriched ASVs were closely related to *Halomicrobiaceae* (particularly *Halomicroarcula*), *Halobacteriales*, *Thermoplasmata*, and *Hadesarchaeota*. There were 182 ASVs enriched in group 3 (lower halite) samples. The most abundant of these ASVs were classified as *Thermoplasmata*. The remaining ASVs are *Halobacteria* from *Halococcus*, *Haloferaceae*, *Halomicrobiaceae*, and *Halobacteriales*.

In the archaeal data set, comparisons between group 3 (lower halite) and group 4 (lower halite and gypsum) samples found no enriched ASVs in either category. In the bacterial data set, these comparisons found 131 enriched ASVs in group 4 and none in group 3. The most abundant of these ASVs are most closely related to *Halapricum*. Other significantly enriched *Halobacteria* in these lower halite and gypsum layers include *Halorussus*, *Halobellus*, and unclassified *Halobacteriales*. ASVs related to *Methanomicrobia*, *Acetothermia*, *Chloroplast*, *Halanerobiales*, *Tepidisphaerales*, and *Desulfobacterales* are also enriched in these sediments.

DISCUSSION

The Bonneville Salt Flats hosts a robust microbial ecosystem. Despite its barren appearance on the surface, the Bonneville Salt Flats (BSF) harbors a robust microbial ecosystem potentially capable of a range of metabolic capabilities, including phototrophy, sulfur and nitrogen cycling metabolisms, and heterotrophy. Although hypersaline systems can be harsh environments for life, they have been previously reported to contain high biomass (17, 24, 25). Our results indicate that BSF is no exception. If we assume 2×10^{-6} ng of DNA per cell, we estimate 10^7 to 10^9 cells per g of sample from our quantifications of environmental DNA. This is likely to be an overestimate because it is known that salt can preserve DNA, and our environmental DNA could include a

significant extracellular fraction (26, 27). In addition, the DNA could also represent eukaryotic species not captured by our 16S rRNA primers. Nevertheless, the low range of our biomass estimate is consistent with other reported values around 10^6 to 10^7 cells ml^{-1} (17, 24, 25).

The surface halite and upper gypsum sediment layers (groups 1 and 2) have higher DNA yields than deeper samples (Table S1). These upper sediments have access to sunlight and oxygen while still retaining protection from UV radiation within the evaporite crusts. In addition, sulfur minerals in the upper gypsum layer likely provide an energy source for chemotrophic microbes living in these upper gypsum layers. Therefore, the upper gypsum layer is likely to have more abundant and more active phototrophic and chemotrophic microbial communities compared to deeper layers.

A microbial community shift occurs along a mineralogical shift in the sediment.

Although the depth of each sediment layer varied per site, microbial communities seemed homogenous among samples within each sediment category. For example, at site 12B, the surface halite was only 3 mm, while at site 56 the surface halite was 25 mm (see Fig. S7 and Data Set S1 in the supplemental material). In spite of these differences in depth, these surface halite samples hosted remarkably similar archaeal and bacterial communities (Fig. S3 and S4). This trend is still evident even between the two samples with the greatest spread between sampling depths: site 12B, where the upper gypsum layer was sampled at a depth of 3 to 7 mm, and site 41, where the gypsum layer was sampled at a depth of 25 to 90 mm. Both of these samples appear similar in mineral classification and relative abundance of microbial taxa. These results suggest microbial communities shift along mineralogical rather than depth gradients at BSF.

Upper halite crusts (group 1) are dominated by heterotrophs from *Salinibacter* and *Halobacteria*. *Halobacteria* gain most of their energy through heterotrophy but are also capable of harnessing sunlight for supplemental ATP production with the specialized pigment bacteriorhodopsin (28–30). *Haloferacaceae* is the dominant family in these upper sediments. Key primary producers in the top halite layer are likely cyanobacteria, particularly *Dactylococcopsis* sp. strain PCC-8305, whose sequences are specifically enriched in these top layers, and the salt-tolerant alga *Dunaliella salina*. Although we did not perform 18S rRNA sequencing to characterize the eukaryotic community, one ASV had 100% identity to the 16S rRNA gene of the *Dunaliella* chloroplast. This ASV was absent at three sites: 12B, 67B, and 41. Sites 12B and 67B had the highest proportion of gypsum for samples in group 1. These sites are also located in a region with the thinnest surface halite (Fig. S7).

Thin sections show that surface halite (group 1) contains large pore spaces and fluid inclusions within the halite crystals (Fig. 1). This upper phototrophic community at BSF likely resides in tandem with heterotrophs in the pore spaces of the halite crystals or as a filamentous biofilm attached to the surfaces of halite crystals (31). Microbes in this surface layer may also be encapsulated within fluid inclusions. Members of this community are likely most active during the flooding stage of BSF, when upper halite dissolves and brine exists on the surface. They may become encapsulated as the brine precipitates into halite crystals during the evaporation period.

Our results indicate that more taxonomic groups are enriched in the upper gypsum sediments (group 2) found beneath the surface halite layer than in other types of sediment (Fig. 2). The higher surface area of clay minerals present in these samples likely provides a more suitable substrate for growth than the surface halite. *Bacteroidetes*, which are often associated with the rhizosphere in other less-extreme soils, are interestingly enriched in this layer (32). Microbes may be concentrated in this layer because gypsum, halite, and other evaporite minerals provide some protection from harsh environmental conditions (such as UV radiation and extreme temperature fluctuations) while still transmitting enough sunlight to support photosynthesis (33). Phototrophs enriched in upper gypsum sediments include members of *Rhodovibrio*, the purple nonsulfur bacteria. In this layer, we also observe abundant sequences related to *Geitlerinema* sp. PCC 9228, which has been shown in cultures to switch between

oxygenic photosynthesis and anoxygenic photosynthesis using sulfide as an electron donor (34).

In general, bacterial taxa associated with sulfur metabolisms (e.g., *Thiohalorhabdus*, *Desulfovermiculus*, *Desulfobacterales*, and *Halanaerobium*) are enriched in the upper gypsum (group 2) layer. These results are strongly suggestive that the abundant sulfur minerals found in this layer (Table 1 and Data Set S1) are metabolized and cycled by the resident microbes. Interestingly, methanogens and acetogens, which often compete with sulfate-reducing bacteria, are also enriched in the upper gypsum layer (35). Methanogens in salt flats often utilize methylated compounds, rather than carbon dioxide, allowing them to coexist with acetogens and sulfate-reducing bacteria (36).

The lower halite and mixed halite and gypsum sediments (groups 3 and 4) contain chemoheterotrophic (*Thermoplasmata* and *Phycisphaeraceae*) and fermentative taxa, perhaps dependent on primary production of the phototrophic community in upper layers. *Bradymonadaceae* (whose type genus was recently described as a facultative anaerobe) and *Tepidisphaerales* (whose type genus was recently described as a facultative aerobe) become enriched again in these lower sediments, suggesting that the transition to a more anaerobic environment occurs at these depths ranging from 15 to 120 mm (37, 38). Aerobic heterotrophs from the *Proteobacteria*, such as *Acinetobacter* and *Oligoflexales*, are also enriched here, although they are low in abundance. This suggests that oxygen may not be completely depleted everywhere at these depths. The dissolution pipes and larger grain sizes found in the lower halite and lower halite mixed with gypsum layers may enable more air and fluid circulation in these sediments (Fig. S2).

The microbial community of BSF is similar to previously described hypersaline ecosystems. Only one culture-independent study of microorganisms at the BSF has been conducted previously (39). This study focused on the adjacent basin Pilot Valley but also included one sampling location at the BSF. The genus *Halolamina* was the most dominant member of the *Halobacteria* in this BSF sample. *Halolamina* sequences were also identified in all of our samples, but the most abundant *Halobacteria* genera in our data set were *Halomicroarcula* and *Halapricum* (Fig. S3 and S4). Culture-dependent studies at BSF have only been successful at isolating *Haloarcula*, *Halorubrum*, *Halobacterium*, and *Salicola* species (40, 41). We also found ASVs with low abundance most closely related to each of these species in our data sets.

The microbial diversity at BSF is comparable to that of other dry saline environments. Archaeal communities are often dominated by members of *Halobacteria* (42–44). Bacterial communities are often dominated by *Bacteroidetes* (*Salinibacter*) and *Proteobacteria* (45–47). Members from *Crenarchaeota*, *Gemmatimonadetes*, *Verrucomicrobia*, SRB from *Deltaproteobacteria*, and *Clostridia* are also commonly reported (48–50). We found ASVs at BSF that are closely related to all of these commonly reported species (Fig. S3 and S4). *Euhalothece* is the most commonly reported dominant cyanobacterium in hypersaline environments (31, 45, 47, 49–52). All of our *Cyanobacteria* ASVs classified within the oxygenic phototrophic class *Oxyphotobacteria*, but we found the oxygenic/anoxygenic *Geitlerinema* sp. PCC 9228 to be the most dominant *Cyanobacteria* at BSF.

Interestingly, many of these same microbial taxa have also been reported in hypersaline lake environments, such the Great Salt Lake, Lake Chaka, and the Salton Sea (51–57), suggesting physiological and/or ecological connections between hypersaline aquatic and evaporite systems.

Conclusions. The Bonneville Salt Flats hosts thriving microbial communities dominated by diverse *Halobacteriaceae* and *Salinibacter* species that are adapted to the challenges of this extreme ecosystem. Many of the archaeal and bacterial taxa are most abundant beneath the halite crust within the upper gypsum sediments, where microbes are likely metabolizing sulfur-containing minerals and can still rely on light penetration for phototrophy.

This study represents the first comprehensive culture-independent characterization of the microbial communities inhabiting the Bonneville Salt Flats, and future work in this understudied ecosystem could address gaps in knowledge, such as which microbes in this ecosystem are crucial for the cycling of nutrients like sulfur and nitrogen, whether haloarchaea are dependent on light filtered through the surface halite crust, how the microbial community shifts with seasonal desiccation and flooding stages, and whether anthropogenic use of this environment for racing and brine mining changed the microbial composition of the ecosystem.

Answering these questions would extend our understanding of the presence and preservation of life not only in extreme environments but also in any environment where salt deposits are formed. Halite crystal growth bands can preserve microbial life present in the original air-water and water-sediment interfaces where the salt formed thousands to hundreds of millions of years ago (13, 58). Evaporite ecosystems may even reflect life on Earth prior to the Cambrian explosion (15). Furthermore, because evaporite deposits on other planetary bodies, such as Mars, are evidence of past or present water (59–62), further advances in the characterization of live and preserved microbes in salt deposits will have implications for the development of extraterrestrial life detection strategies.

MATERIALS AND METHODS

Sampling location and collection. Samples were collected from eight pits dug with sterile tools in September 2016 (Data Set S1 and Fig. S1). Distinct sediment layers visually identified by color and textural changes were sampled at each site. Samples were immediately placed on ice and transported within 12 h to the University of Utah, where they were stored at -80°C until microbiological analyses were performed in the following 6 months.

Elemental and sedimentological analysis. A portion of each homogenized sample was separated and analyzed for major and trace elements by ActLabs. Major and trace elements were analyzed via Aqua Regia ICP (Inductively Coupled Plasma, method 1E3). Anions were analyzed via ion chromatography (method 6B). Using these elemental data, along with visual characteristics, each sample was grouped into one of four sediment categories. Elemental concentrations were used to reconstruct relative weight mineralogy based upon stoichiometry of gypsum, halite, silicates, and other detrital minerals. Elemental concentrations beyond detection limits were derived using this method.

In addition to these samples, additional blocks of representative material were collected at the same time of sampling from sites 56, 35, and 12B. These blocks were processed by Wagner Petrographic to create petrographic thin sections for visual microscopy analysis. Blocks were desiccated to remove any pore waters and impregnated with clear or colored epoxy. Several thin sections were made from each block by cutting 50- by 75-mm blocks and mounting them on glass slides. Samples were cut to thicknesses ranging from 0.5 to 2 mm. The samples were then analyzed at the University of Utah using an Olympus BX53M microscope with $\times 1,000$ magnification and a Zeiss M2 petroscopic microscope with an Axiocam camera and Zen 2 Pro software.

DNA extraction and sequencing. DNA was extracted from salt crust samples using a protocol from Brazelton et al. (63) modified for highly saline material. The modified protocol is available on our lab's website (<https://baas-becking.biology.utah.edu/data/category/18-protocols>) and summarized here. Sediment samples were crushed and homogenized with a sterile mortar and pestle, and 0.25-g subsamples were placed in a DNA extraction buffer containing 0.1 M Tris, 0.1 M EDTA, 0.1 M KH_2PO_4 , 0.8 M guanidium HCl, and 0.5% Triton X-100. For lysis, samples were subjected to one freeze-thaw cycle, incubation at 65°C for 30 min, and beating with 0.1-mm glass beads in a Mini-Beadbeater-16 (Biospec Products). Purification was performed via extraction with phenol-chloroform-isoamyl alcohol, precipitation in ethanol, washing in Amicon 30K Ultra centrifugal filters, and final cleanup with $2\times$ SPRI beads (64). DNA quantification was performed with a Qubit fluorometer (Thermo Fisher).

Archaeal and bacterial 16S rRNA gene amplicon sequencing was conducted by the Michigan State University genomics core facility. The V4 region of the bacterial 16S rRNA gene was amplified with dual-indexed Illumina fusion primers with the 515F/806R primers, as described by Kozich et al. (65). The V4 region of the archaeal 16S rRNA gene was amplified with the A519F/Arch958R primers (66). Amplicon concentrations were normalized and pooled using an Invitrogen SequelPrep DNA Normalization Plate. After library QC and quantitation, the pool was loaded on an Illumina MiSeq v2 flow cell and sequenced using a standard 500 cycle reagent kit. Base calling was performed by Illumina real-time analysis (RTA) using software v1.18.54. The RTA output was demultiplexed and converted to fastq files using Illumina Bcl2fastq v1.8.4.

Analysis of 16S rRNA amplicon data. Quality screening and processing of all 16S rRNA amplicon sequences was conducted with the DADA2 R package (67). Using this package, primer contaminants and chimeras were removed, reads were trimmed and filtered based on quality, and sequence variants likely to be derived by sequencing error were identified. The final amplicon sequence variants (ASVs) are considered to be true variants and are analyzed in the same method as traditional operational taxonomic

units. The taxonomic classification of all ASVs was performed with the DADA2 package and the SILVA reference database (NRv132).

Sequence counts for each ASV were transformed with a biomass correction by multiplying the proportion of each ASV's contribution to each sample's total sequence count by the estimated number of total cells in that sample. The total cells were estimated by using the total amount (in ng) of extracted DNA (as measured by the Qubit fluorometer) and an assumption of 2×10^{-6} ng of DNA per cell. All downstream analyses were performed with these biomass-weighted relative abundances. Differential abundance of ASVs in each layer was performed using edgeR (23) and phyloseq (68). edgeR was used to determine the FDR using the Benjamini-Hochberg method. An ASV was considered to be significantly enriched in a layer if its differential abundance passed an FDR threshold of 0.05. Multivariate analysis was done using phyloseq (68), and Bray-Curtis and Simpson indices were calculated using vegan (69).

Data availability. All sequence data are publicly available at the NCBI Sequence Read Archive under BioProject [PRJNA522308](https://doi.org/10.5281/zenodo.2827066). All SRA metadata, full supplementary material, and protocols are archived at <https://doi.org/10.5281/zenodo.2827066>. All custom software and scripts are available at <https://github.com/Brazelton-Lab>.

SUPPLEMENTAL MATERIAL

Supplemental material for this article may be found at <https://doi.org/10.1128/mSphere.00378-19>.

FIG S1, TIF file, 1.8 MB.

FIG S2, TIF file, 2.7 MB.

FIG S3, TIF file, 1.2 MB.

FIG S4, TIF file, 0.6 MB.

FIG S5, TIF file, 0.7 MB.

FIG S6, TIF file, 1.1 MB.

FIG S7, TIF file, 1.3 MB.

TABLE S1, DOCX file, 0.02 MB.

TABLE S2, DOCX file, 0.01 MB.

DATA SET S1, XLSX file, 0.4 MB.

ACKNOWLEDGMENTS

This research was supported by the National Science Foundation Award 1617473 (CNH-L: Adaptation, Mitigation, and Biophysical Feedbacks in the Changing Bonneville Salt Flats).

We thank Emily Dart and Betsy Kleba for assistance with sample collection, DNA extraction, and general insight on the BSF system. We also thank Alex Hyer and Christopher Thornton for computational assistance.

REFERENCES

- Crittenden MD. 1963. New data on the isostatic deformation of Lake Bonneville. *Geol Surv Prof*, paper 454-E.
- Noeth LA. 2002. Bonneville: the fastest place on earth. MBI Publishing Company, St. Paul, MN.
- Eardley AJ. 1962. Gypsum dunes and evaporite history of the Great Salt Lake Desert. *Utah Geol Mineral Surv*, special study 2.
- Turk LJ. 1970. Evaporation of brine: a field study on the Bonneville Salt Flats, Utah. *Water Resour Res* 6:1209–1215. <https://doi.org/10.1029/WR006i004p01209>.
- Turk LJ, Davis SN, Bingham CP. 1973. Hydrogeology of lacustrine sediments, Bonneville Salt Flats, Utah. *Econ Geol* 68:65–78. <https://doi.org/10.2113/gsecongeo.68.1.65>.
- Lines GC. 1979. Hydrology and surface morphology of the Bonneville Salt Flats and Pilot Valley Playa, Utah. *Geol Surv Water-Supply*, paper 2057.
- White WW, III, Terrazas M. 2006. Analysis of recent and historical salt-crust thickness measurements and assessment of their relationship to the salt laydown project, Bonneville Salt Flats, Tooele County, Utah. *Utah Geological Association publication* 34. Utah Geological Association, Salt Lake City, UT.
- Kaliser BM. 1967. Bonneville Salt Flats hydrogeological study near Wendover, Utah, Spring 1967.
- Brooks SJ. 1991. A comparison of salt thickness on the Bonneville Salt Flats, Tooele County, Utah during July 1960, October 1974, and October 1988.
- Bowen BB, Bernau J, Kipnis EL, Lerback J, Wetterlin L, Kleba B. 2018. The making of a perfect racetrack at the Bonneville Salt Flats. *Sed Record* 16:4–11. <https://doi.org/10.2110/sedred.2018.2.4>.
- Bowen BB, Kipnis EL, Pechmann JM. 2018. Observations of salt crust thickness change at the Bonneville Salt Flats from 2003–2016, p 247–285. *In* *Geofluids of Utah*. Utah Geological Association publication 47. Utah Geological Association, Salt Lake City, UT.
- Bowen BB, Benison KC. 2009. Geochemical characteristics of naturally acid and alkaline saline lakes in southern Western Australia. *Appl Geochem* 24:268–284. <https://doi.org/10.1016/j.apgeochem.2008.11.013>.
- Lowenstein TK, Hardie LA. 1985. Criteria for the recognition of salt-pan evaporites. *Sedimentology* 32:627–644. <https://doi.org/10.1111/j.1365-3091.1985.tb00478.x>.
- Bowen BB, Kipnis EL, Raming LW. 2017. Temporal dynamics of flooding, evaporation, and desiccation cycles and observations of salt crust area change at the Bonneville Salt Flats, Utah. *Geomorphology* 299:1–11. <https://doi.org/10.1016/j.geomorph.2017.09.036>.
- Ventosa A, de la Haba RR, Sánchez-Porro C, Papke RT. 2015. Microbial diversity of hypersaline environments: a metagenomic approach. *Curr Opin Microbiol* 25:80–87. <https://doi.org/10.1016/j.mib.2015.05.002>.
- Ma Y, Galinski EA, Grant WD, Oren A, Ventosa A. 2010. Halophiles 2010: life in saline environments. *Appl Environ Microbiol* 76:6971–6981. <https://doi.org/10.1128/AEM.01868-10>.
- Litchfield C, Gillevet P. 2002. Microbial diversity and complexity in hy-

- persaline environments: a preliminary assessment. *J Ind Microbiol Biotechnol* 28:48–55. <https://doi.org/10.1038/sj/jim/7000175>.
18. Oren A. 1999. Bioenergetic aspects of halophilism. *Microbiol Mol Biol Rev* 63:334–348.
 19. Ventosa A, Nieto JJ. 1995. Biotechnological applications and potentialities of halophilic microorganisms. *World J Microbiol Biotechnol* 11: 85–94. <https://doi.org/10.1007/BF00339138>.
 20. Parada AE, Needham DM, Fuhrman JA. 2016. Every base matters: assessing small subunit rRNA primers for marine microbiomes with mock communities, time series and global field samples. *Environ Microbiol* 18:1403–1414. <https://doi.org/10.1111/1462-2920.13023>.
 21. Walters W, Hyde ER, Berg-Lyons D, Ackermann G, Humphrey G, Parada A, Gilbert JA, Jansson JK, Caporaso JG, Fuhrman JA, Apprill A, Knight R. 2015. Transcribed spacer marker gene primers for microbial community surveys. *mSystems* 1:1. <https://doi.org/10.1128/mSystems.00009-15>.
 22. Apprill A, McNally S, Parsons R, Weber L. 2015. Minor revision to V4 region SSU rRNA 806R gene primer greatly increases detection of SAR11 bacterioplankton. *Aquat Microb Ecol* 75:129–137. <https://doi.org/10.3354/ame01753>.
 23. McMurdie PJ, Holmes S. 2013. edgeR: a bioconductor package for differential expression analysis of digital gene expression data. *Genome Res* 8:4.
 24. Çınar S, Mutlu MB. 2016. Comparative analysis of prokaryotic diversity in solar salterns in eastern Anatolia (Turkey). *Extremophiles* 20:589–601. <https://doi.org/10.1007/s00792-016-0845-7>.
 25. Maturrano L, Santos F, Rosselló-Mora R, Antón J. 2006. Microbial diversity in Maras salterns, a hypersaline environment in the Peruvian Andes. *Appl Environ Microbiol* 72:3887–3895. <https://doi.org/10.1128/AEM.02214-05>.
 26. Rhodes ME, Spear JR, Oren A, House CH. 2011. Differences in lateral gene transfer in hypersaline versus thermal environments. *BMC Evol Biol* 11:199. <https://doi.org/10.1186/1471-2148-11-199>.
 27. Borin S, Crotti E, Mapelli F, Tamagnini I, Corselli C, Daffonchio D. 2008. DNA is preserved and maintains transforming potential after contact with brines of the deep anoxic hypersaline lakes of the Eastern Mediterranean Sea. *Saline Systems* 4:10. <https://doi.org/10.1186/1746-1448-4-10>.
 28. Hartmann R, Sickinger HD, Oesterhelt D. 1980. Anaerobic growth of halobacteria. *Proc Natl Acad Sci U S A* 77:3821–3825. <https://doi.org/10.1073/pnas.77.7.3821>.
 29. Spudich JL. 1998. Variations on a molecular switch: transport and sensory signalling by archaeal rhodopsins. *Mol Microbiol* 28:1051–1058. <https://doi.org/10.1046/j.1365-2958.1998.00859.x>.
 30. Sharma AK, Walsh DA, Bapteste E, Rodriguez-Valera F, Ford Doolittle W, Papke RT. 2007. Evolution of rhodopsin ion pumps in haloarchaea. *BMC Evol Biol* 7:79. <https://doi.org/10.1186/1471-2148-7-79>.
 31. Spear JR, Ley RE, Berger AB, Pace NR. 2003. Complexity in natural microbial ecosystems: the Guerrero Negro experience. *Biol Bull* 204: 168–173. <https://doi.org/10.2307/1543553>.
 32. Mendes R, Garbeva P, Raaijmakers JM. 2013. The rhizosphere microbiome: significance of plant beneficial, plant pathogenic, and human pathogenic microorganisms. *FEMS Microbiol Rev* 37:634–663. <https://doi.org/10.1111/1574-6976.12028>.
 33. Friedmann EI. 1982. Endolithic microorganisms in the Antarctic cold desert. *Science* 215:1045–1053. <https://doi.org/10.1126/science.215.4536.1045>.
 34. Grim SL, Dick GJ. 2016. Photosynthetic versatility in the genome of *Geitlerinema* sp. PCC 9228 (formerly *Oscillatoria limnetica* 'solar lake'), a model anoxygenic photosynthetic cyanobacterium. *Front Microbiol* 7:1546. <https://doi.org/10.3389/fmicb.2016.01546>.
 35. Kato S, Yoshida R, Yamaguchi T, Sato T, Yumoto I, Kamagata Y. 2014. The effects of elevated CO₂ concentration on competitive interaction between acetate- and syntrophic methanogenesis in a model microbial consortium. *Front Microbiol* 5:575.
 36. García-Maldonado JQ, Bebout BM, Everroad RC, López-Cortés A. 2015. Evidence of novel phylogenetic lineages of methanogenic *Archaea* from hypersaline microbial mats. *Microb Ecol* 69:106–117. <https://doi.org/10.1007/s00248-014-0473-7>.
 37. Wang ZJ, Liu QQ, Zhao LH, Du ZJ, Chen GJ. 2015. *Bradymonas sediminis* gen. nov., sp. nov., isolated from coastal sediment, and description of *Bradymonadaceae* fam. nov. and *Bradymonadales* ord. nov. *Int J Syst Evol Microbiol* 65:1542–1549. <https://doi.org/10.1099/ijs.0.000135>.
 38. Kovaleva OL, Merkel AY, Novikov AA, Baslerov RV, Toshchakov SV, Bonch-Osmolovskaya EA. 2015. *Tepidisphaera mucosa* gen. nov., sp. nov., a moderately thermophilic member of the class *Phycisphaerae* in the phylum *Planctomycetes*, and proposal of a new family, *Tepidisphaeraceae* fam. nov., and a new order, *Tepidisphaerales* ord. nov. *Int J Syst Evol Microbiol* 65:549–555. <https://doi.org/10.1099/ijs.0.070151-0>.
 39. Lynch KL. 2015. A geobiological investigation of the hypersaline sediments of Pilot Valley, Utah: a terrestrial analog to ancient lake basins on Mars. Colorado School of Mines, Golden, CO.
 40. Boogaerts GL. 2015. Preliminary characterization of the microbial community in the Bonneville Salt Flats. The University of Alabama—Birmingham, Birmingham, AL.
 41. King GM. 2015. Carbon monoxide as a metabolic energy source for extremely halophilic microbes: implications for microbial activity in Mars regolith. *Proc Natl Acad Sci U S A* 112:4465–4470. <https://doi.org/10.1073/pnas.1424989112>.
 42. Kambourova M, Tomova I, Boyadzhieva I, Radchenkova N, Vasileva-Tonkova E. 2017. Phylogenetic analysis of the bacterial community in a crystallizer pond, Pomorie salterns, Bulgaria. *Biotechnol Biotechnol Equip* 31:325–332. <https://doi.org/10.1080/13102818.2016.1265900>.
 43. Di Meglio L, Santos F, Gomariz M, Almansa C, López C, Antón J, Nercessian D. 2016. Seasonal dynamics of extremely halophilic microbial communities in three Argentinian salterns. *FEMS Microbiol Ecol* 92:1–15.
 44. Stivaletta N, Barbieri R, Picard C, Bosco M. 2009. Astrobiological significance of the sabkha life and environments of southern Tunisia. *Planet Space Sci* 57:597–605. <https://doi.org/10.1016/j.pss.2008.10.002>.
 45. Stivaletta N, Barbieri R, Cevenini F, López-García P. 2011. Physicochemical conditions and microbial diversity associated with the evaporite deposits in the Laguna de la Piedra (Salar de Atacama, Chile). *Geomicrobiol J* 28:83–95. <https://doi.org/10.1080/01490451003653102>.
 46. Rasuk MC, Kurth D, Flores MR, Contreras M, Novoa F, Poire D, Farias ME. 2014. Microbial characterization of microbial ecosystems associated with evaporite domes of gypsum in Salar de Llamara in Atacama Desert. *Microb Ecol* 68:483–494. <https://doi.org/10.1007/s00248-014-0431-4>.
 47. Vogt JC, Abed RMM, Albach DC, Palinska KA. 2018. Bacterial and archaeal diversity in hypersaline cyanobacterial mats along a transect in the intertidal flats of the Sultanate of Oman. *Microb Ecol* 75:331–347. <https://doi.org/10.1007/s00248-017-1040-9>.
 48. Kim JS, Makama M, Petito J, Park NH, Cohan FM, Dungan RS. 2012. Diversity of *Bacteria* and *Archaea* in hypersaline sediment from Death Valley National Park, California. *Microbiol Open* 1:135–148. <https://doi.org/10.1002/mbo3.20>.
 49. Caton IR, Schneegurt MA. 2012. Culture-independent analysis of the soil bacterial assemblage at the Great Salt Plains of Oklahoma. *J Basic Microbiol* 52:16–26. <https://doi.org/10.1002/jobm.201100175>.
 50. McKay CP, Rask JC, Detweiler AM, Bebout BM, Everroad RC, Lee JZ, Chanton JP, Mayer MH, Caraballo AAL, Kapili B, Al-Awar M, Al-Farraj A. 2016. An unusual inverted saline microbial mat community in an inter-dune Sabkha in the Rub' al Khali (the Empty Quarter), United Arab Emirates. *PLoS One* 11:e0150342. <https://doi.org/10.1371/journal.pone.0150342>.
 51. Schneider D, Arp G, Reimer A, Reitner J, Daniel R. 2013. Phylogenetic analysis of a microbialite-forming microbial mat from a hypersaline lake of the Kiritimati Atoll, Central Pacific. *PLoS One* 8:e66662. <https://doi.org/10.1371/journal.pone.0066662>.
 52. Lindsay MR, Anderson C, Fox N, Scofield G, Allen J, Anderson E, Bueter L, Poudel S, Sutherland K, Munson-McGee JH, Van Nostrand JD, Zhou J, Spear JR, Baxter BK, Lageson DR, Boyd ES. 2017. Microbialite response to an anthropogenic salinity gradient in Great Salt Lake, Utah. *Geobiology* 15:131–145. <https://doi.org/10.1111/gbi.12201>.
 53. Swan BK, Ehrhardt CJ, Reifel KM, Moreno LI, Valentine DL. 2010. Archaeal and bacterial communities respond differently to environmental gradients in anoxic sediments of a California hypersaline lake, the Salton Sea. *Appl Environ Microbiol* 76:757–768. <https://doi.org/10.1128/AEM.02409-09>.
 54. Bowman JP, McCammon SA, Rea SM, McMeekin TA. 2000. The microbial composition of three limnologically disparate hypersaline Antarctic lakes. *FEMS Microbiol Lett* 183:81–88. <https://doi.org/10.1111/j.1574-6968.2000.tb08937.x>.
 55. Dillon JG, Carlin M, Gutierrez A, Nguyen V, McLain N. 2013. Patterns of microbial diversity along a salinity gradient in the Guerrero Negro solar saltern, Baja CA Sur, Mexico. *Front Microbiol* 4:399. <https://doi.org/10.3389/fmicb.2013.00399>.
 56. Jiang H, Dong H, Yu B, Liu X, Li Y, Ji S, Zhang CL. 2007. Microbial response to salinity change in Lake Chaka, a hypersaline lake on Tibetan

- plateau. *Environ Microbiol* 9:2603–2621. <https://doi.org/10.1111/j.1462-2920.2007.01377.x>.
57. Almeida-Dalmet S, Sikaroodi M, Gillevet P, Litchfield C, Baxter B. 2015. Temporal study of the microbial diversity of the north arm of Great Salt Lake, Utah, U.S. *Microorganisms* 3:310–326. <https://doi.org/10.3390/microorganisms3030310>.
 58. Sankaranarayanan K, Lowenstein TK, Timofeeff MN, Schubert BA, Lum JK. 2014. Characterization of ancient DNA supports long-term survival of *Haloarchaea*. *Astrobiology* 14:553–560. <https://doi.org/10.1089/ast.2014.1173>.
 59. Douglas S. 2005. Mineralogical footprints of microbial life. *Am J Sci* 305:503–525. <https://doi.org/10.2475/ajs.305.6-8.503>.
 60. Barbieri R, Stivaletta N. 2011. Continental evaporites and the search for evidence of life on Mars. *Geol J* 46:513–524. <https://doi.org/10.1002/gj.1326>.
 61. Rothschild LJ. 1990. Earth analogs for Martian life: microbes in evaporites, a new model system for life on Mars. *Icarus* 88:246–260. [https://doi.org/10.1016/0019-1035\(90\)90188-F](https://doi.org/10.1016/0019-1035(90)90188-F).
 62. Barbieri R, Stivaletta N. 2012. Halophiles, continental evaporites and the search for biosignatures in environmental analogues for Mars, p 13–26. *In* *Life on earth and other planetary bodies*. Springer, Dordrecht, Netherlands.
 63. Brazelton WJ, Ludwig KA, Sogin ML, Andreishcheva EN, Kelley DS, Shen C-C, Edwards RL, Baross JA. 2010. Archaea and bacteria with surprising microdiversity show shifts in dominance over 1,000-year time scales in hydrothermal chimneys. *Proc Natl Acad Sci U S A* 107:1612–1617. <https://doi.org/10.1073/pnas.0905369107>.
 64. Rohland N, Reich D. 2012. Cost-effective, high-throughput DNA sequencing libraries for multiplexed target capture. *Genome Res* 22:939–946. <https://doi.org/10.1101/gr.128124.111>.
 65. Kozich JJ, Westcott SL, Baxter NT, Highlander SK, Schloss PD. 2013. Development of a dual-index sequencing strategy and curation pipeline for analyzing amplicon sequence data on the MiSeq Illumina sequencing platform. *Appl Environ Microbiol* 79:5112–5120. <https://doi.org/10.1128/AEM.01043-13>.
 66. Klindworth A, Pruesse E, Schweer T, Peplies J, Quast C, Horn M, Glöckner FO. 2013. Evaluation of general 16S ribosomal RNA gene PCR primers for classical and next-generation sequencing-based diversity studies. *Nucleic Acids Res* 41:1.
 67. Callahan BJ, McMurdie PJ, Rosen MJ, Han AW, Johnson AJA, Holmes SP. 2016. DADA2: high-resolution sample inference from Illumina amplicon data. *Nat Methods* 13:581–587. <https://doi.org/10.1038/nmeth.3869>.
 68. McMurdie PJ, Holmes S. 2013. Phyloseq: an R package for reproducible interactive analysis and graphics of microbiome census data. *PLoS One* 8:e61217. <https://doi.org/10.1371/journal.pone.0061217>.
 69. Oksanen J, Guillaume Blanchet F, Friendly M, Kindt R, Legendre P, McGlenn D, Minchin PR, O'Hara RB, Simpson GL, Solymos P, Stevens MHH, Wagner H. 2018. vegan: community ecology package. R package, v2.5-2.